Response to Referee #3

The authors numerically investigate collisions of charged cloud droplets and rain drops, accounting for influence of atmospheric electric field. For this purpose, they first calculate collision efficiency table considering gravity force, drag forces and electrical forces acting on drops in course of their interaction. Corresponding drop motion equations are formulated using superposition method and are integrated using second order Runge-Kutta method. Then authors solve stochastic collection equation (SCE) for 2D drop size distribution (DSD), where the first independent variable is drop mass and the second the drop charge. SCE is solved for various initial DSDs, charges and electric field strengths. Authors conclude that "electric field could significantly enhance the collision process" in the case when the initial DSD is given in the range of small cloud droplets. I would like to note that theory and methods used by the authors in their research are not new (all the needed references are given in the study). Nevertheless, the results obtained in the study are of interest so I recommend the manuscript for publication in ACP after major revision.

1. The English language of the manuscript is of a very low quality. Please find a way to enhance it in order to render the text more readable and comprehensible.

Response: Thanks for the reviewer's comment on the writing of the paper. We have substantially revised the whole manuscript. The Introduction of the manuscript is completely rewritten. Most part of the Results, Abstract, and Conclusion are rewritten. Description of the methods are now improved in writing. The whole manuscript is now more organized and more readable. We have also checked the grammar throughout the manuscript. Grammar errors and unclear sentences are all changed. In the response to reviewer's 2nd comment, we show part of the rewritten Introduction to summarize the electrification process in clouds. In the response to reviewer's 12th comment, we show the rewritten section 5.1, where the electrostatic effects on collision efficiency is discussed.

2. It is worth explaining in the introduction how charges appear in cloudy drops.

Response: Yes, it is necessary to explain the charging process in clouds. At the beginning of the rewritten Introduction, we use two paragraphs to explain the electrification in thunderstorms and in warm clouds. These paragraphs now read as:

Clouds are usually electrified (Pruppacher and Klett 1997). For thunderstorms, several theories of electrification have been proposed in the past decades. The proposed theories assume that the electrification involves the collision of graupel or hailstones with ice crystals or supercooled cloud droplets, based on radar observational result that the onset of strong electrification follows the formation of graupel or hailstones within the cloud (Wallace and Hobbs, 2006). However, the exact conditions and mechanisms are still under debate. One charging process could be due to the thermoelectric effect between the rimed and relatively warm graupel or hailstones with the relatively cold ice crystals or supercooled cloud droplets. Another charging process could be due to the polarization of particles by the downward atmospheric electric field. The thunderstorm electrification can increase the electric fields to several thousand V cm^{-1}, while the magnitude of electric fields in fair

weather air is only about 1 V cm^{-1} (Pruppacher and Klett 1997). Droplet charges can reach $|q| \approx 42r^2$ in unit of elementary charge in thunderstorms, with the droplet radius r in unit of μm according to observations (Takahashi, 1973).

Liquid stratified clouds do not have such strong charge generation as in the thunderstorms. But charging of droplets can indeed occur at the upper and lower cloud boundaries as the fair weather current passes through the clouds (Harrison et al. 2015, Baumgaertner et al. 2014). The global fair weather current and the electric field are in the downward direction. Given the electric potential of 250 kV for the ionosphere, the exact value of fair weather current density over a location depends on the electric resistance of the atmospheric column, but its typical value is about 2×10^{-12} A m^{-2} (Baumgaertner et al. 2014). The fair weather electric field is typically about 1 V cm^{-1} in the cloud-free air, but is usually much stronger inside stratus clouds, because the cloudy air has a lower electrical conductivity than the cloud-free air. There is a conductivity transition at cloud boundaries. Therefore, the cloud top is positively charged and the cloud base is negatively charged. Based on the in situ measurements of charge density in liquid stratified cloud, and assuming that the cloud has a droplet number concentration on the order of 100 cm^{-3}, it is estimated that the mean charge per droplet is +5e (ranging from +1e to +8e) at cloud top, and -6e (ranging from -1e to -16e) at cloud base. Other studies found different amount of charges in clouds. According to Tsutomu Takahashi (1973) and Khain (1997), the mean absolute charge of droplets in warm clouds is around $|q| \approx 6.6\ r^{1.3}$ (with units of e and μm for q and r, respectively). For a droplet with radii of 10 μm, it is about 131 e.

New references:

Tsutomu Takahashi: Measurement of electric charge of cloud droplets, drizzle, and raindrops, Reviews of Geophysics and Space Physics,11, 903-924, 1973
Harrison, R. G., Nicoll, K. A., Ambaum, M. H. P.: On the microphysical effects of observed cloud edge charging, Q. J. R. Meteorol. Soc., 141, 2690–2699, doi:10.1002/qj.2554, 2015
Baumgaertner, A. J. G., Lucas, G. M., Thayer, J. P., Mallios, S. A.: On the role of clouds in the fair weather part of the global electric circuit, Atmos. Chem. Phys., 14, 8599–8610, doi:10.5194/acp-14-8599-2014, 2014
Wallace, J. M., Hobbs, P. V.: Atmospheric Science, Second Edition, Academic Press, 2006

3. Line 123: Suddenly, the concept of "no-slip boundary conditions" appear. To explain.

Response: Thanks for the reviewer to point this out. An explanation is added to the manuscript. Before line 115, the following paragraph is added. (In the revised manuscript, U is the droplet velocity relative to the fluid.)

Both Stokes and Hamielec stream functions satisfy the no-slip boundary condition, which means that the fluid at the droplet boundary has zero velocity relative to the droplet. Hamielec stream function is no-slip because those functions $A_1, \ldots, B_4$ in Eq. (5b) satisfy $A_1 + 2A_2 + 3A_3 + 4A_4 = 1$ and $B_1 + 2B_2 + 3B_3 + 4B_4 = 0$, as long as the droplet is considered as a rigid sphere (Hamielec, 1963). These relations ensure that $u_\theta = -U \sin\theta$ at the surface of the droplet. Note that u_θ is the velocity of fluid at the surface, and $U \sin\theta$ is the tangential velocity of the droplet surface. The two velocities are equal, which ensures the no-slip boundary condition.

4. To illustrate Eqs. (11) and (12) by a figure. To show directions of all the forces acting on drops and the velocities of the drops.

Response: Thanks for the reviewer's comment. Equation (11) represents the force acting on droplet 2, due to the charge of droplet 1 and the external electric field. We now changed the order of the last two terms in the first line of equation (11), so that the first three terms in the first line represent the force in the radial direction due to the external electric field, and the fourth term in the first line represents the force in the radial direction due to the charge of droplet 1. The second line of Equation (11) represents the force in the tangential direction due to the electric field.
The equation now is:

$$\boldsymbol{F}_{e2} = \{r_2{}^2 E_0^2 (F_1 \cos^2\theta + F_2 \sin^2\theta) + E_0 \cos\theta (F_3 q_1 + F_4 q_2) + E_0 q_2 \cos\theta + \frac{1}{r_2^2}(F_5 q_1{}^2 + F_6 q_1 q_2 + F_7 q_2{}^2)\}\hat{\boldsymbol{e}}_{\boldsymbol{R}}$$
$$+ \{r_2{}^2 E_0^2 F_8 \sin 2\theta + E_0 \sin\theta (F_9 q_1 + F_{10} q_2) + E_0 q_2 \sin\theta\}\hat{\boldsymbol{e}}_{\boldsymbol{\theta}}$$

When the electric field E_0 is zero, the equation is reduced to

$$\boldsymbol{F}_{e2} = \frac{1}{r_2^2}(F_5 q_1{}^2 + F_6 q_1 q_2 + F_7 q_2{}^2)\hat{\boldsymbol{e}}_{\boldsymbol{R}}$$

This equation describes the force due to the charge in droplet 1. We have added the above new equation to the manuscript. In Figure 2 of the original manuscript, the force from the conductor model is indeed based on the equation above. In Figure 2, this conductor model is compared with the inverse-square law as described by Equation (10).

The figure below shows the forces acting on droplet 1 and droplet 2, and the velocities of the droplets. It has been added to the revised manuscript as Figure 3. These forces are terms on the right hand side of Eq. 4, including gravity force, flow drag force, and electrostatic force. Note that the electrostatic force $\boldsymbol{F}_{e1}$, $\boldsymbol{F}_{e2}$ include two parts: the electric force from the other droplet (F_{inter} in the figure), and the force from the external electric field ($E_0 q_1$ in the figure). When considering the two droplets as a system, the electric force from the other droplet can be considered as internal force. The velocity of droplet 2 is usually not straightly downward, because it tends to follow the streamlines when approaching with droplet 1.

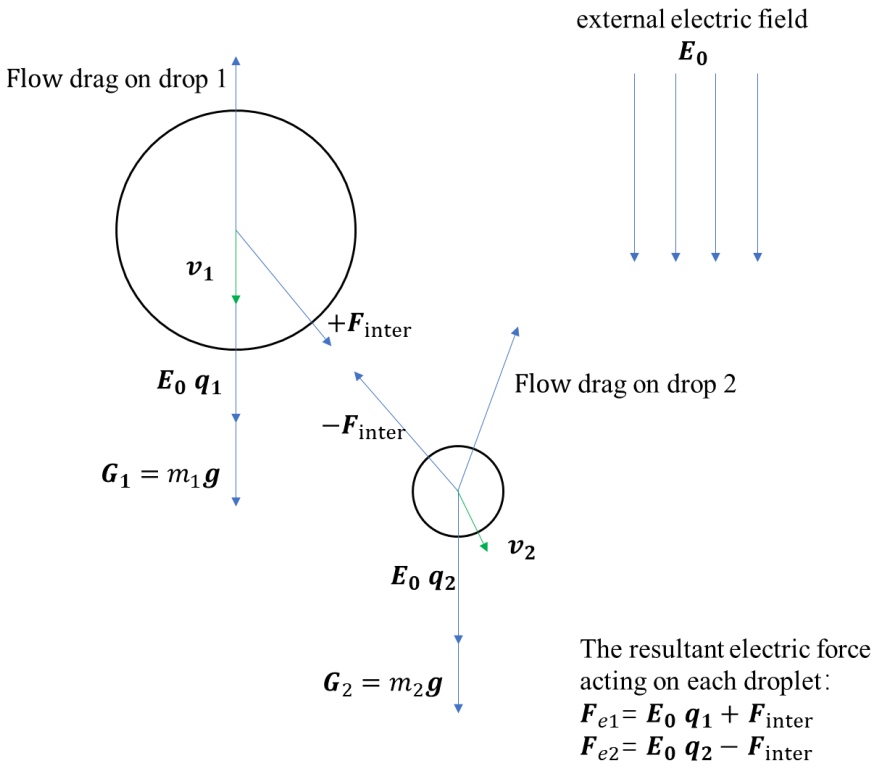

5. Is it right that appear in the Eq. (12)?

Response: Yes it is right. We should have emphasized that F_{e1} and F_{e2} consist not only the electric force from the other droplet, but also the force from the external electric field. As mentioned in the response to reviewer's 4th comment, the order of two terms in Equation (11) is changed, so that it is easier to identify the force due to the external electric field and the force due to the charge in the other droplet. Because the two droplets can be considered as a system, the sum of the forces they experience independently ($F_{e1} + F_{e2}$) must be equal to the external electric force acting on the system $E_0(q_1 + q_2)\hat{e}_z$. This relation is expressed in equation (12). If we have already known F_{e2}, then F_{e1} is derived immediately from Eq. (12). In line 140 of the original manuscript, we have made some changes in the writing of the manuscript to explain this.

6. Line 153: actually, you integrate the system of 12 (or 8) equations

Response: Thanks for the reviewer's careful reading. We have added this information to the manuscript based on reviewer's comment.

7. Line 187: Eq. (13) is the exponential distribution and not the gamma distribution.

Response: Yes Eq. (13) is the exponential distribution. Thanks to the reviewer for pointing this out. We have made the correction in the manuscript. We should mention that Eq. (14) and (15) are gamma distributions. Please refer to the response to the 8th comment for detailed discussions on how to obtain Eq. (15).

8. How did you obtain Eq. (15) from Eq. (14)?

Response:

Thanks for this question. We now have added more information to this part, so that it is easier to understand the equations for size distribution. Basically, definitions of the size distribution is used for the derivation. Recall that $n(m)$ is the droplet number concentration per unit mass interval, and $M(m)$ is the mass concentration per unit mass interval.

The distribution of droplet number concentration $n(m)$ can also be written as $n(r)$, or $n(\ln r)$. We know that the definition of $n(m)$ is: $n(m) = \mathrm{d}N/\mathrm{d}m$, where $\mathrm{d}m$ is the mass interval, and $\mathrm{d}N$ is the droplet number concentration in that mass interval. $n(r) = \mathrm{d}N/\mathrm{d}r$ represents the droplet number concentration per unit size interval. $n(\ln r) = \mathrm{d}N/\mathrm{d}\ln r$ represents droplet number concentration per unit interval of logarithmic size. Similarly, the distribution of droplet mass concentration $M(m)$ can be written as $M(r)$, and $M(\ln r)$. These functions are related together.
$M(\ln r)$ and $M(r)$ are related through:

$$M(\ln r) = \mathrm{d}M/\mathrm{d}\ln r = r \cdot \mathrm{d}M/\mathrm{d}r = r \cdot M(r)$$

While $M(r)$ can be related with $M(m)$ through:

$$M(m) = \frac{\mathrm{d}M}{\mathrm{d}m} = \frac{1}{4\pi r^2}\frac{\mathrm{d}M}{\mathrm{d}r} = \frac{M(r)}{4\pi r^2}$$

With $m = 4\pi r^3\rho/3$, and assuming that $\bar{m} = 4\pi\bar{r}^3\rho/3$, where $\bar{r}$ is the mean radius, we can obtain $M(\ln r)$ from $M(m)$,

$$M(\ln r) = 3L\frac{r^6}{\bar{r}^6}exp\left(-\frac{r^3}{\bar{r}^3}\right)$$

In the revised manuscript, we added a new equation for $n(\ln r)$, because $n(\ln r)$ is also plotted and discussed in the Results section.

$$n(\ln r) = L\frac{9r^3}{4\pi\bar{r}^6}exp\left(-\frac{r^3}{\bar{r}^3}\right)$$

9. The authors should check the correctness of equations (13-15).

Response: Thanks for the suggestion. We have checked the equations to make sure they are correct.

10. Lines 195-200. To add information about number concentration, liquid water content and charge content for all initial drop spectra.

Response: The initial liquid water content is set to be L=1 g m^{-3}, for all simulations. This is a typical value in warm clouds. The initial averaged droplet radius $\bar{r}$ is set to be 15 μm, 9 μm and 6.5 μm, where $\bar{r} =$ 15 μm case represents the clean conditions (less aerosol), and 6.5 μm represents polluted conditions (more aerosol). These settings give an initial droplet number concentration of 70, 325, and 850 cm^{-3}, respectively. The charge content is set as in the following table. The number concentration and charge content for all initial drop size distribution are shown in table 2 in the revised manuscript.

Table 2. Total number concentration, charge content for the initial droplet size distribution

mean radius $\bar{r}$ (μm)	number concentration N (cm^{-3})	total positive charge Q^+ (e cm^{-3})	total negative charge Q^- (e cm^{-3})
15	70.6	+9384	-9384
9	324.8	+15638	-15638
6.5	850.5	+21634	-21634

Note that the initial droplet number concentration is distributed into different size bins and different charge bins. The size distribution is based on functions described in Equations (13)-(15). The charge distribution is now based on a Gaussian distribution in the revised manuscript, instead of the method described in lines 200-202 in the original manuscript. Ratios shown in lines 200-202 in the original manuscript is an approximation of 2:3:4:3:2, but it is arbitrarily chosen to mimic a normal distribution, and also to satisfy electric neutrality $\bar{q} = 0$. In the revised manuscript, we use a Gaussian distribution to describe droplet distribution over the charge bins.

Lines 199-202 have been revised and it reads as follows in the revised manuscript:

To simulate an early stage of the warm-cloud precipitation, we need to distribute the droplets in each size bin to different charge bins, so that these droplets have different charges. Since there is little data on this, we assume a Gaussian distribution,

$$N(q) = \frac{N}{\sqrt{2\pi}\sigma}\exp\left(-\frac{q^2}{2\sigma^2}\right)$$

where N is the number concentration in the size bin, and σ is the standard deviation of the Gaussian distribution in that bin. $N(q)$ represents the number concentration of droplets with charge q. This distribution satisfies electric neutrality $\bar{q} = 0$. For different size bin, droplet number concentration N is different. We purposely set the standard deviation σ to be different for different size bins. For larger size, the charge amount is larger, based on $\overline{|q|} = 1.31\ r^2$ (q in unit of elementary charge and r in μm) as stated in the Introduction. Therefore, we set larger standard deviation σ for the larger size bins.

11. Line 216: Please add the figure showing collision efficiency between cloud droplets (1-20 μm in radii), the same as in fig. 5. It is all the more important because you obtained the maximal effect for cloud droplets.

Response: As suggested, we plot a new figure below, to show the collision efficiencies for smaller collectors (r_1 = 5, 10, 15, 20 and 25 μm) when the droplet pairs have no charge. X-axis denotes the ratio of radius r_2/r_1. As will be seen in the response to reviewer's 12th comment, the 10 μm and 20 μm lines will be shown together with the results for charged droplets (new Fig. 6). Therefore, we think this figure is not necessary in the manuscript.

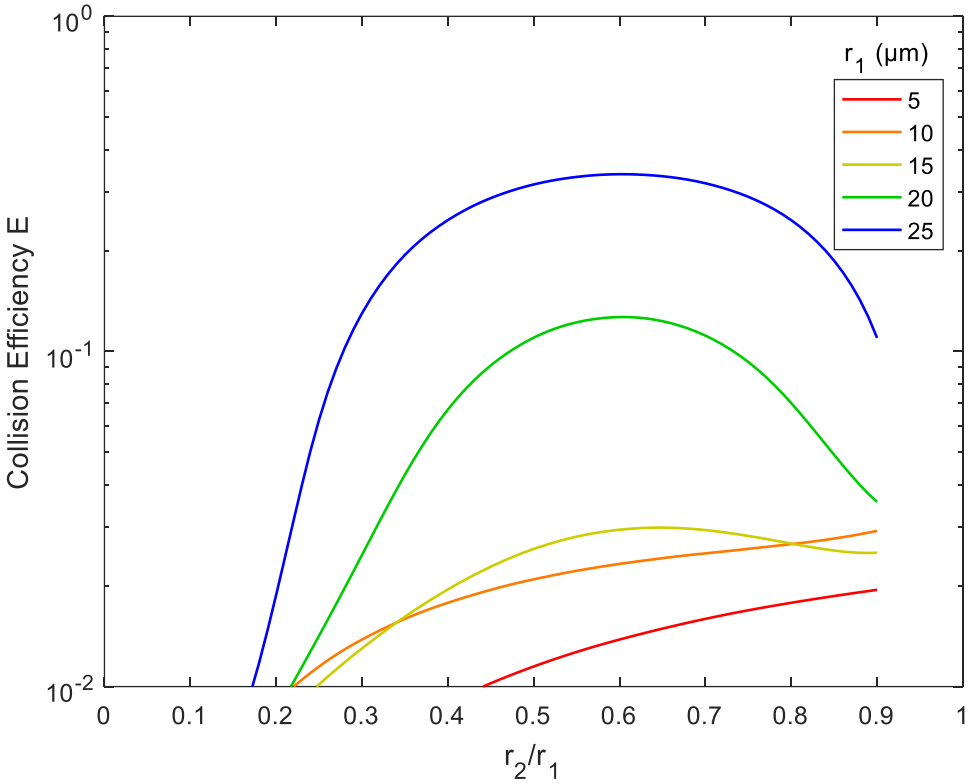

12. Figure 6: Please, add illustrations for different collectors (say 15 ïA¸ m, and 10 ïA¸ m in radii) and comment them.

Response: Thank you very much for the suggestion. As suggested, we have shown the different collectors r_1= 10, 20, 30 and 40 μm in the new figure below. Fig. 6 now describes the collision efficiency for the 30 and 40 μm collectors (precipitating droples). Fig. 7 now describes the collision efficiency for the 10 and 20 μm collectors (cloud droplets). Therefore, section 5.1 has been substantially revised. Most part of it has been rewritten. It is clear that electrostatic effects are significant for small droplets. We show the rewritten section 5.1 here:

5.1 Collision efficiency

Here we present collision efficiencies for typical droplet pairs to illustrate the electrostatic effect. During the evolution of cloud droplet size distribution, the radius and charge amount of colliding droplets have large variability. In addition, the charge sign of the colliding droplets may be the same or the opposite. Therefore, only some examples are shown.

The collision efficiencies for droplet pairs with no electric charge and field is presented in Fig. 5 as a reference. Collector droplets with radii larger than 30 μm are shown here to represent the precipitating droplets. The calculated collision efficiencies from this study are also compared with the measurements from previous studies. It is seen that results from this study are generally consistent with the measurements. Collision efficiencies increase as r_2 changes from 2 to 14 μm, and also increase as r_1 changes from 30 to 305 μm. For two droplets that are both large enough, collision efficiency could be

close to 1.

Figure 6 shows the collision efficiencies for droplet pairs with electric charge and field. The detailed characteristics of the droplet pairs are shown in Table 1. Basically, droplet pairs that have no charge, with same-sign charges, and with opposite-sign charges are selected here, and under the 0 and 400 V m^{-1} electric fields. Results for the collector droplet with a radius of 30 μm (Fig. 6a) and 40 μm (Fig. 6b) are shown. When comparing Fig. 6a and 6b, it can be seen that electrostatic effects are less significant for a larger collector. The electrostatic effects are even weaker for collector radius larger than 40 μm (figures not shown). Therefore, we use the 30 μm collector as an example to explain the electrostatic effects on collision efficiencies below.

For the collector droplet with a radius of 30 μm (Fig. 6a), noticeable, and sometimes significant electrostatic effect can be seen. Compared to the droplet pair with no charge (line 1), the positively-charged pair under no electric field (line 2) has a slightly smaller collision efficiency, due to the repulsive force. As can be seen in Fig. 2, when the charged droplets move together, they first experience repulsive force, then attractive force at small distance. The integrated effect is that the droplets have smaller collision efficiency. The results for negatively-charged pair under no electric field are identical to line 2 and therefore are not shown. When a downward electric field of 400 V m^{-1} is added, the positively-charged pair (line 3) has a collision efficiency very close to the pair with no charge. This implies that the enhancement of collision efficiency by the electric field offsets the repulsive force effect. For a negatively-charged pair in a downward electric field (line 4), the collision efficiency with small r_2 is significantly enhanced. This could be easily explained by electrostatic induction: the strong downward electric field induces positive charge on the lower part of the collector droplet (even though it is overall negatively-charged), so the negative-charged collected droplet below experiences attractive force.

As for a pair with opposite-sign charges, line 5 in Fig. 6a shows that the collision efficiency is enhanced by the electrostatic effect even when there is no electric field. The collision efficiency is nearly an order of magnitude higher with $r_2 < 5$ μm. Line 6 in Fig. 6a shows that, with an electric field of 400 V cm^{-1}, the electrostatic effect for the pairs with opposite-sign charges is even stronger. There is also an interesting feature in Fig. 6a: as the collector and collected droplets have similar sizes, collision efficiency is high for the pairs with opposite-sign charges. This is quite different from the other four lines, where collision efficiencies are very low for droplet pairs with similar sizes.

Figure 7 shows the collision efficiencies for droplet pairs with charge and field, with smaller collectors. The collector droplet has a radius of 10 μm (Fig. 7a) and 20 μm (Fig. 7b) here, and can be used to represent cloud droplets. Collision efficiencies for these smaller collectors are much smaller than 1 when there is no charge (line 1 in Figs. 7a and 7b), which is already well known in cloud physics community. However, the electrostatic effects are so strong that the collision efficiencies could be significantly changed for these collectors. For the collector droplet with a radius of 10 μm (Fig. 7a), the positively-charged pair has a very small collision efficiency that is out of the scale in the figure, due to the dominating effect of the repulsive force as discussed above. For the positively-charged pair under a downward electric field, the collision efficiencies is on the similar order of magnitude as the pair with no charge. For the negatively-charged pair under the downward electric field, and for the pairs with opposite-sign charges, the electrostatic effects is very strong. The negatively-charged pair even has the collision efficiency increased by two orders of magnitude. Similarly, for the collector

droplet with a radius of 20 μm (Fig. 7b), the electrostatic effect can lead to an order of magnitude increase in collision efficiencies.

It is evident that droplet charge and field can significantly affect collision efficiency, especially for smaller collectors. This means that the electrostatic effects depend on the radius of collector droplets, and mainly affects small droplets. The section below provides a detailed description on how these electrostatic effects can influence droplet size distributions.

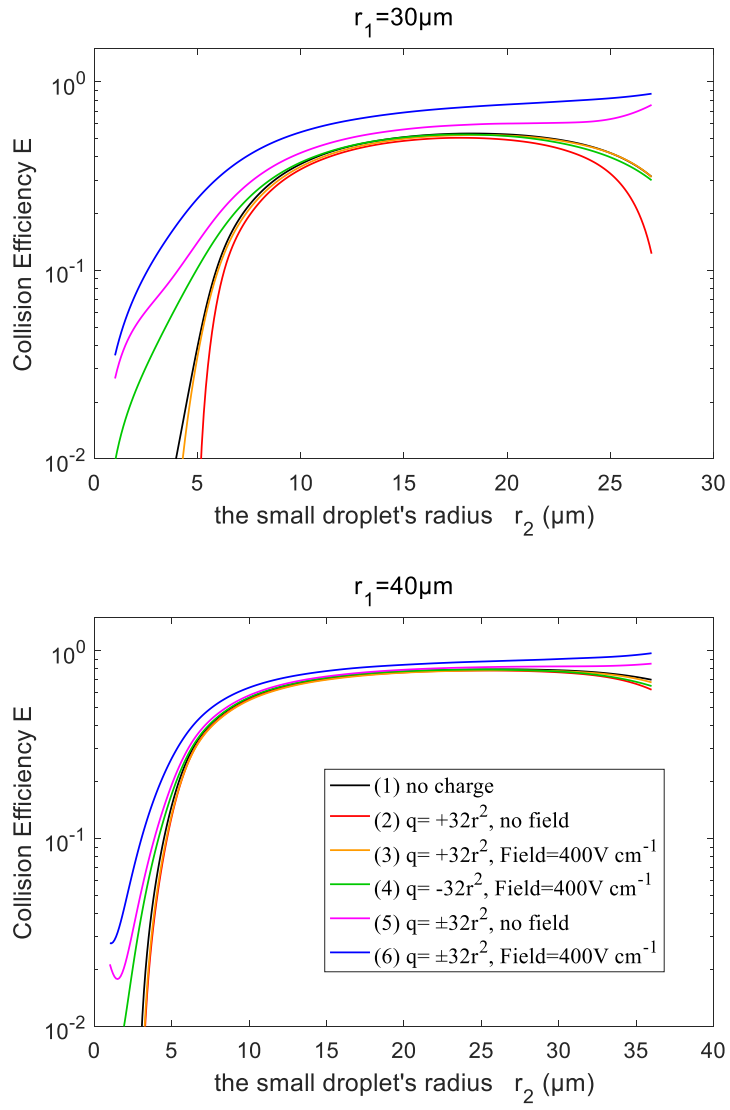

FIG. 6. Collision efficiency for droplets with electric charge and field. The radius of the collector droplet r_1 is: (a) 30.0 μm, (b) 40.0 μm . X-axis denotes the collected droplet raidus r_2. The two droplets carry electric charges proportional to r^2. The lines for droplet pairs with no charge (line 1 in Fig. 6a and 6b) are the same as the 30 μm and 40 μm lines in Fig. 5.

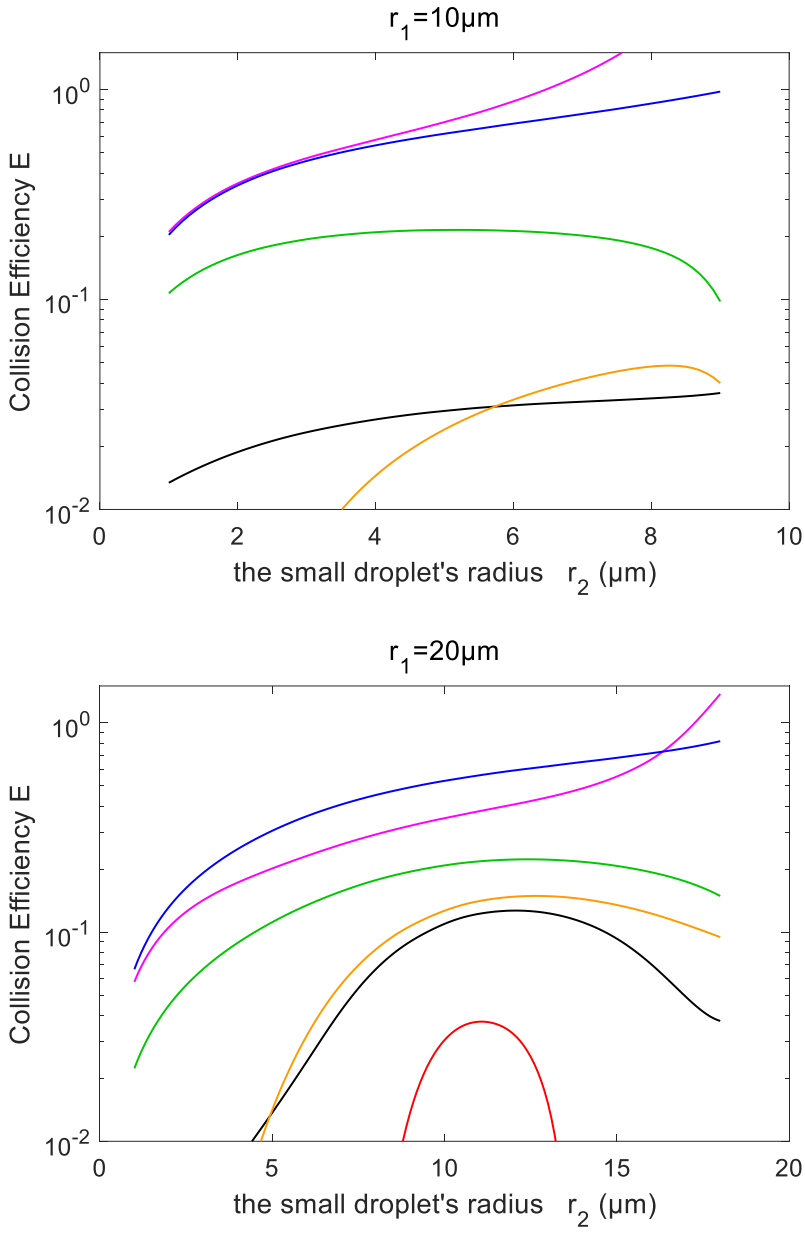

FIG. 7. Collision efficiency for droplets with electric charge and field. The radius of the collector droplet r_1 is: (a) 10.0 μm, (b) 20.0 μm. The other characteristics of the droplet pairs are similar to those in Fig. 6.

13. Section 5.2: Please show temporal changes of drop concentration and charge content and comment on them. How fast the charges of opposite signs compensate each other?

Response: Thanks for the reviewer's suggestion. The evolution of droplet concentration and charge

content are shown in the below. These figures are also added to the manuscript as new Fig. 9, 11, and 14.

From Fig. 9 ($\bar{r}$ =15 μm), it is evident that droplet concentrations in the 4 different electric conditions decrease from about 70 cm^{-3} to less than 5 cm^{-3}, and the evolution is nearly not affected by the electric conditions. The electrostatic effect is therefore negligible in this case.

From Fig. 11 ($\bar{r}$ =9 μm), we can see the evolution is distinctly affected by the 4 different electric conditions. Electric charges and fields play an important role in converting smaller droplets to larger droplets, and decreasing the droplet number concentration.

From Figure 14 ($\bar{r}$ =6.5 μm), droplet concentration is strongly affected by the 4 different electric conditions. Results show that the electric field would remarkably trigger the collision-coalescence process for the small droplets.

Comparing the upper and lower panels of each figure, it is evident that the charges of opposite signs compensate each other as fast as the decrease of number concentration (except for the uncharged case). The phases of charge neutralizations are the same as changes of drop concentration. In all the three figures, more than 90% charges of opposite signs are neutralized during the evolution.

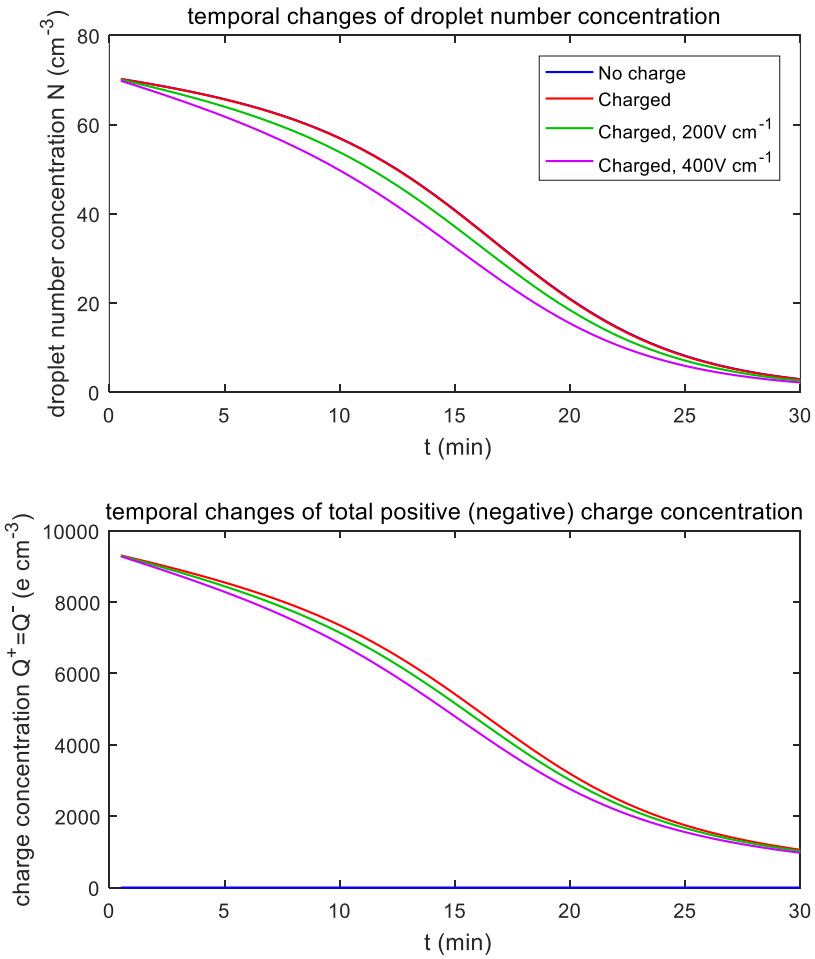

FIG. 9. Temporal changes of droplet total number concentration and total charge content for $\bar{r}$ =15 μm.

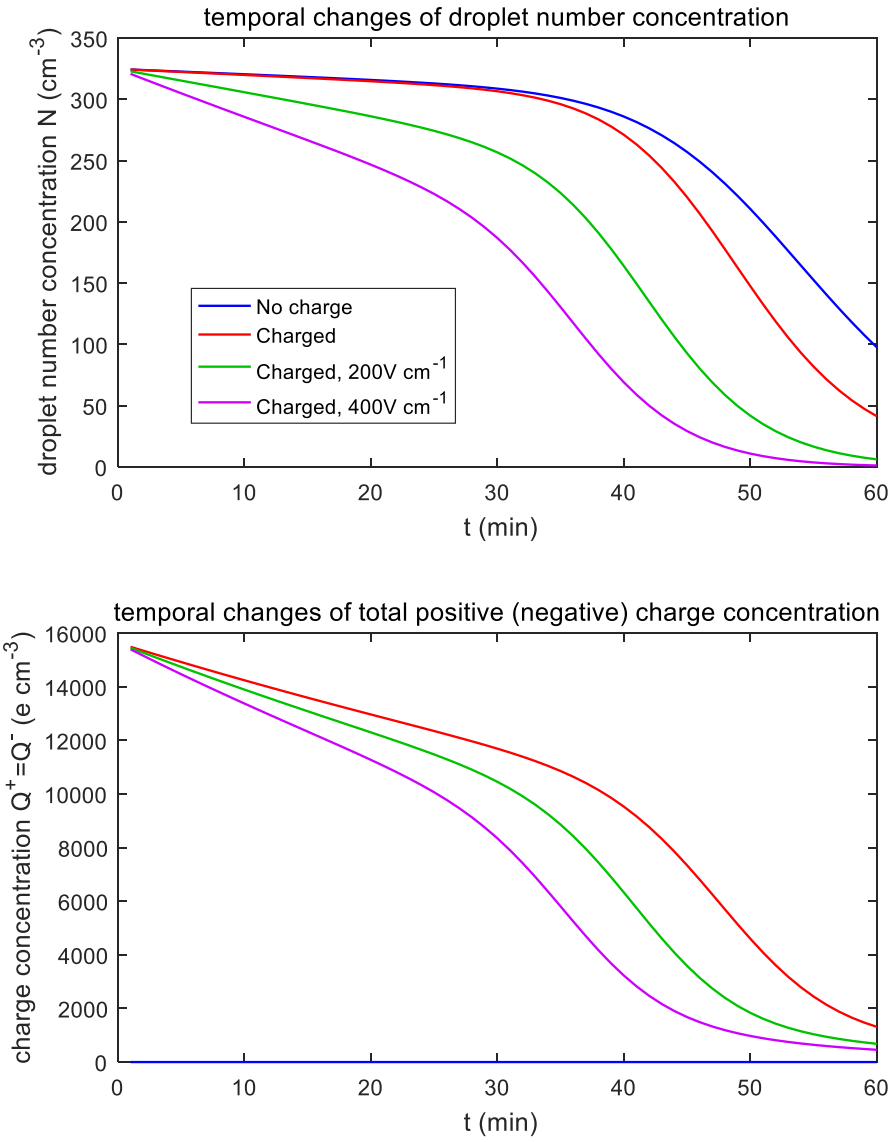

FIG. 11. Temporal changes of droplet total number concentration and total charge content for $\bar{r}$ =9 μm

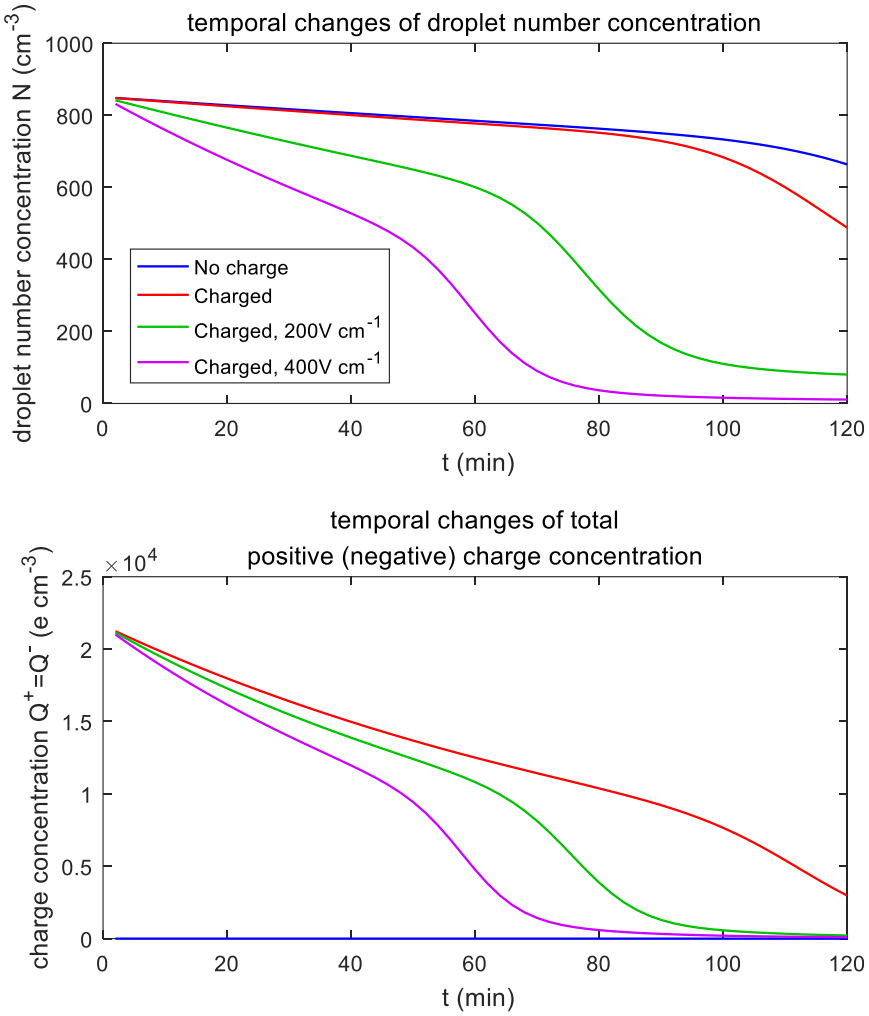

FIG. 14. Temporal changes of droplet total number concentration and total charge content for $\bar{r}$ =6.5 μm.

14. Line 288: "The relative terminal velocity term also contributes to the collection kernel, and the electric field can affect terminal velocity of small charged droplets significantly." – Please, cover this issue in more detail in the article.

Response: Thanks for the reviewer's suggestion. We have improved the writing of this part
Lines 287-295 "The electric enhancement of…" have been revised to:
However, the relative terminal velocity term also contributes to the collection kernel, which is shown in Eq. (2). As mentioned above, terminal velocities $\boldsymbol{V_1}$ or $\boldsymbol{V_2}$ are derived by simulating just single one charged droplet in air with certain electric field, and letting it fall until its velocity converges to the terminal velocity. Therefore, the electric field can affect terminal velocities of charged droplets, thus to affect the collection kernels. Terminal velocities of droplets in an external electric field is illustrated in Fig. 15. In downwards electric field 400 V cm^{-1}, terminal velocity of a large droplet is

hardly affected. The difference of velocity caused by electric field at $r =$ 1000 μm does not exceed 1%, and the one at 100 μm does not exceed 5%. On the contrary, electric fields strongly affect the terminal velocities of charged small droplets. For r < 5 μm, the terminal velocities of negative-charged droplets even turn "upwards", namely the electric field lifts them up in the air. Electric fields mainly affect terminal velocities of small charged droplets, because droplet mass $m \propto r^3$, while droplet charge $q \propto r^2$ according to observation. So, $q \propto m^{2/3}$ means that acceleration contributed by electric force decreases with increasing droplet mass, which explain that the terminal velocity of small charged droplets is more sensitive to the electric field.

In Fig.11 of the original manuscript, y-axis is in logarithmic scale and stands for the absolute value of terminal velocity, which is ambiguous. In the revised manuscript, we plot the negative terminal velocity in a separate panel, as shown below. (The whole manuscript has been revised substantially, so it becomes Fig. 15 now)

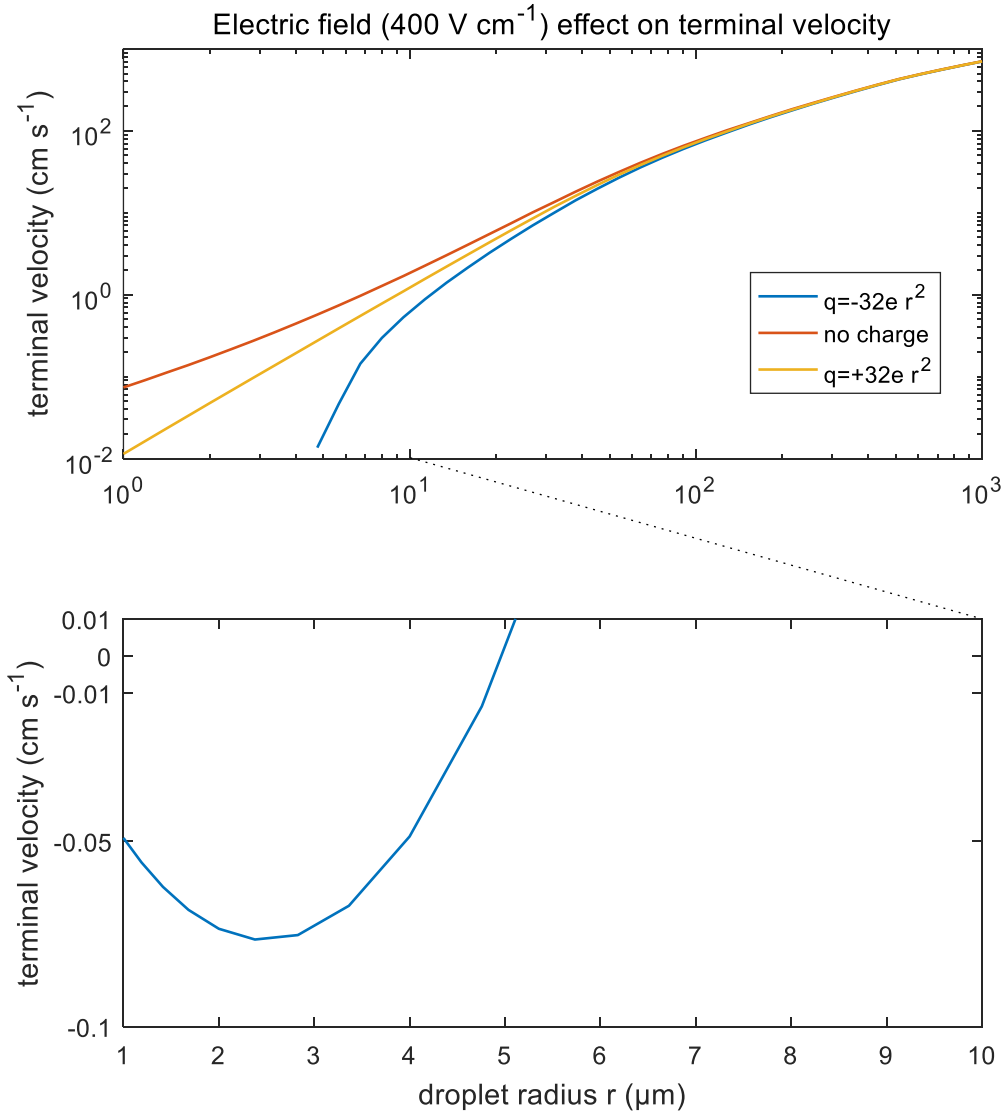

Figure 15. Terminal velocities of droplets in an external electric field 400 V cm^{-1}. Different lines denote different droplet charge conditions. It is seen that the terminal velocity of negatively-charged droplets

smaller than 5 μm would turn upwards, which leads to the discontinuity of the lower curve in the figure.